



Measurement of the Ratio of b Quark Production Cross Sections in $\bar{p}p$ Collisions
at $\sqrt{s} = 630$ GeV and $\sqrt{s} = 1800$ GeV

D. Acosta,¹³ T. Affolder,²⁴ H. Akimoto,⁴⁷ M. G. Albrow,¹² D. Ambrose,³⁴ D. Amidei,²⁶ K. Anikeev,²⁵ J. Antos,¹ G. Apollinari,¹² T. Arisawa,⁴⁷ A. Artikov,¹⁰ T. Asakawa,⁴⁵ W. Ashmanskas,⁹ F. Azfar,³² P. Azzi-Bacchetta,³³ N. Bacchetta,³³ H. Bachacou,²⁴ W. Badgett,¹² S. Bailey,¹⁷ P. de Barbaro,³⁸ A. Barbaro-Galtieri,²⁴ V. E. Barnes,³⁷ B. A. Barnett,²⁰ S. Baroiant,⁵ M. Barone,¹⁴ G. Bauer,²⁵ F. Bedeschi,³⁵ S. Belforte,⁴⁴ W. H. Bell,¹⁶ G. Bellettini,³⁵ J. Bellinger,⁴⁸ D. Benjamin,¹¹ J. Bensinger,⁴ A. Beretvas,¹² J. P. Berge,¹² J. Berryhill,⁹ A. Bhatti,³⁹ M. Binkley,¹² D. Bisello,³³ M. Bishai,¹² R. E. Blair,² C. Blocker,⁴ K. Bloom,²⁶ B. Blumenfeld,²⁰ S. R. Blusk,³⁸ A. Bocci,³⁹ A. Bodek,³⁸ G. Bolla,³⁷ Y. Bonushkin,⁶ D. Bortoletto,³⁷ J. Boudreau,³⁶ A. Brandl,²⁸ S. van den Brink,²⁰ C. Bromberg,²⁷ M. Brozovic,¹¹ E. Brubaker,²⁴ N. Bruner,²⁸ E. Buckley-Geer,¹² J. Budagov,¹⁰ H. S. Budd,³⁸ K. Burkett,¹⁷ G. Busetto,³³ A. Byon-Wagner,¹² K. L. Byrum,² S. Cabrera,¹¹ P. Calafiura,²⁴ M. Campbell,²⁶ W. Carithers,²⁴ J. Carlson,²⁶ D. Carlsmith,⁴⁸ W. Caskey,⁵ A. Castro,³ D. Cauz,⁴⁴ A. Cerri,³⁵ A. W. Chan,¹ P. S. Chang,¹ P. T. Chang,¹ J. Chapman,²⁶ C. Chen,³⁴ Y. C. Chen,¹ M. -T. Cheng,¹ M. Chertok,⁵ G. Chiarelli,³⁵ I. Chirikov-Zorin,¹⁰ G. Chlachidze,¹⁰ F. Chlebana,¹² L. Christofek,¹⁹ M. L. Chu,¹ J. Y. Chung,³⁰ Y. S. Chung,³⁸ C. I. Ciobanu,³⁰ A. G. Clark,¹⁵ A. P. Colijn,¹² A. Connolly,²⁴ M. Convery,³⁹ J. Conway,⁴⁰ M. Cordelli,¹⁴ J. Cranshaw,⁴² R. Culbertson,¹² D. Dagenhart,⁴⁶ S. D'Auria,¹⁶ F. DeJongh,¹² S. Dell'Agnello,¹⁴ M. Dell'Orso,³⁵ S. Demers,³⁸ L. Demortier,³⁹ M. Deninno,³ P. F. Derwent,¹² T. Devlin,⁴⁰ J. R. Dittmann,¹² A. Dominguez,²⁴ S. Donati,³⁵ J. Done,⁴¹ M. D'Onofrio,³⁵ T. Dorigo,¹⁷ N. Eddy,¹⁹ K. Einsweiler,²⁴ J. E. Elias,¹² E. Engels, Jr.,³⁶ R. Erbacher,¹² W. Erdmann,¹² D. Errede,¹⁹ S. Errede,¹⁹ Q. Fan,³⁸ S. Farrington,¹⁶ H.-C. Fang,²⁴ R. G. Feild,⁴⁹ J. P. Fernandez,¹² C. Ferretti,³⁵ R. D. Field,¹³ I. Fiori,³ B. Flaughner,¹² G. W. Foster,¹² M. Franklin,¹⁷ J. Freeman,¹² J. Friedman,²⁵ T. A. Fuess,² Y. Fukui,²³ I. Furic,²⁵ S. Galeotti,³⁵ A. Gallas,²⁹ M. Gallinaro,³⁹ T. Gao,³⁴ M. Garcia-Sciveres,²⁴ A. F. Garfinkel,³⁷ P. Gatti,³³ C. Gay,⁴⁹ D. W. Gerdes,²⁶ E. Gerstein,⁸ P. Giannetti,³⁵ P. Giromini,¹⁴ V. Glagolev,¹⁰ D. Glenzinski,¹² M. Gold,²⁸ J. Goldstein,¹² I. Gorelov,²⁸ A. T. Goshaw,¹¹ Y. Gotra,³⁶ K. Goulios,³⁹ C. Green,³⁷ G. Grim,⁵ P. Gris,¹² C. Grosso-Pilcher,⁹ M. Guenther,³⁷ G. Guillian,²⁶ J. Guimaraes da Costa,¹⁷ R. M. Haas,¹³ C. Haber,²⁴ S. R. Hahn,¹² C. Hall,¹⁷ T. Handa,¹⁸ R. Handler,⁴⁸ W. Hao,⁴² F. Happacher,¹⁴ K. Hara,⁴⁵ A. D. Hardman,³⁷ R. M. Harris,¹² F. Hartmann,²¹ K. Hatakeyama,³⁹ J. Hauser,⁶ J. Heinrich,³⁴ A. Heiss,²¹ M. Hennecke,²¹ M. Herndon,²⁰ C. Hill,⁵ A. Hocker,³⁸ K. D. Hoffman,⁹ R. Hollebeek,³⁴ L. Holloway,¹⁹ B. T. Huffman,³² R. Hughes,³⁰ J. Huston,²⁷ J. Huth,¹⁷ H. Ikeda,⁴⁵ J. Incandela,¹² * G. Introzzi,³⁵ A. Ivanov,³⁸ J. Iwai,⁴⁷ Y. Iwata,¹⁸ E. James,²⁶ M. Jones,³⁴ U. Joshi,¹² H. Kambara,¹⁵ T. Kamon,⁴¹ T. Kaneko,⁴⁵ M. Karagoz Unel,²⁹ K. Karr,⁴⁶ S. Kartal,¹² H. Kasha,⁴⁹ Y. Kato,³¹ T. A. Keaffaber,³⁷ K. Kelley,²⁵ M. Kelly,²⁶ R. D. Kennedy,¹² R. Kephart,¹² D. Khazins,¹¹ T. Kikuchi,⁴⁵ B. Kilminster,³⁸ B. J. Kim,²² D. H. Kim,²² H. S. Kim,¹⁹ M. J. Kim,⁸ S. B. Kim,²² S. H. Kim,⁴⁵ Y. K. Kim,²⁴ M. Kirby,¹¹ M. Kirk,⁴ L. Kirsch,⁴ S. Klimenko,¹³ P. Koehn,³⁰ K. Kondo,⁴⁷ J. Konigsberg,¹³ A. Korn,²⁵ A. Korytov,¹³ E. Kovacs,² J. Kroll,³⁴ M. Kruse,¹¹ S. Krutelyov,⁴¹ S. E. Kuhlmann,² K. Kurino,¹⁸ T. Kuwabara,⁴⁵ A. T. Laasanen,³⁷ N. Lai,⁹ S. Lami,³⁹ S. Lammel,¹² J. Lancaster,¹¹ M. Lancaster,²⁴ R. Lander,⁵ A. Lath,⁴⁰ G. Latino,²⁸ T. J. LeCompte,² K. Lee,⁴² S. Leone,³⁵ J. D. Lewis,¹² M. Lindgren,⁶ T. M. Liss,¹⁹ J. B. Liu,³⁸ T. Liu,¹² Y. C. Liu,¹ D. O. Litvintsev,¹² O. Lobban,⁴² N. S. Lockyer,³⁴ J. Loken,³² M. Loretto,³³ D. Lucchesi,³³ P. Lukens,¹² S. Lusin,⁴⁸ L. Lyons,³² J. Lys,²⁴ R. Madrak,¹⁷ K. Maeshima,¹² P. Maksimovic,¹⁷ L. Malferrari,³ M. Mangano,³⁵ G. Manca,³² M. Mariotti,³³ G. Martignon,³³ A. Martin,⁴⁹ V. Martin,²⁹ J. A. J. Matthews,²⁸ P. Mazzanti,³ K. S. McFarland,³⁸ P. McIntyre,⁴¹ M. Menguzzato,³³ A. Menzione,³⁵ P. Merkel,¹² C. Mesropian,³⁹ A. Meyer,¹² T. Miao,¹² R. Miller,²⁷ J. S. Miller,²⁶ H. Minato,⁴⁵ S. Miscetti,¹⁴ M. Mishina,²³ G. Mitselmakher,¹³ Y. Miyazaki,³¹ N. Moggi,³ E. Moore,²⁸ R. Moore,²⁶ Y. Morita,²³ T. Moulik,³⁷ M. Mulhearn,²⁵ A. Mukherjee,¹² T. Muller,²¹ A. Munar,³⁵ P. Murat,¹² S. Murgia,²⁷ J. Nachtman,⁶ V. Nagaslaev,⁴² S. Nahn,⁴⁹ H. Nakada,⁴⁵ I. Nakano,¹⁸ C. Nelson,¹² T. Nelson,¹² C. Neu,³⁰ D. Neuberger,²¹ C. Newman-Holmes,¹² C.-Y. P. Ngan,²⁵ H. Niu,⁴ L. Nodulman,² A. Nomerotski,¹³ S. H. Oh,¹¹ Y. D. Oh,²² K. Ohl,⁴⁹ T. Ohmoto,¹⁸ T. Ohsugi,¹⁸ R. Oishi,⁴⁵ T. Okusawa,³¹ J. Olsen,⁴⁸ W. Orejudos,²⁴ C. Pagliarone,³⁵ F. Palmonari,³⁵ R. Paoletti,³⁵ V. Papadimitriou,⁴² S. Pappas,⁴⁹ D. Partos,⁴ J. Patrick,¹² G. Pauletta,⁴⁴ M. Paulini,⁸ C. Paus,²⁵ D. Pellett,⁵ L. Pescara,³³ T. J. Phillips,¹¹ G. Piacentino,³⁵ K. T. Pitts,¹⁹ A. Pompos,³⁷ L. Pondrom,⁴⁸ G. Pope,³⁶ T. Pratt,³² F. Prokoshin,¹⁰ J. Proudfoot,² F. Ptohos,¹⁴ O. Pukhov,¹⁰ G. Punzi,³⁵ A. Rakitine,²⁵ F. Ratnikov,⁴⁰ D. Reher,²⁴ A. Reichold,³² P. Renton,³² A. Ribon,³³ W. Riegler,¹⁷ F. Rimondi,³ L. Ristori,³⁵ M. Riveline,⁴³ W. J. Robertson,¹¹ T. Rodrigo,⁷ S. Rolli,⁴⁶ L. Rosenson,²⁵ R. Roser,¹² R. Rossin,³³ C. Rott,³⁷ A. Roy,³⁷ A. Ruiz,⁷ A. Safonov,⁵ R. St. Denis,¹⁶ W. K. Sakumoto,³⁸ D. Saltzberg,⁶ C. Sanchez,³⁰ A. Sansoni,¹⁴ L. Santi,⁴⁴ H. Sato,⁴⁵ P. Savard,⁴³ A. Savoy-Navarro,¹² P. Schlabach,¹² E. E. Schmidt,¹² M. P. Schmidt,⁴⁹

M. Schmitt,²⁹ L. Scodellaro,³³ A. Scott,⁶ A. Scribano,³⁵ A. Sedov,³⁷ S. Segler,¹² S. Seidel,²⁸ Y. Seiya,⁴⁵
 A. Semenov,¹⁰ F. Semeria,³ T. Shah,²⁵ M. D. Shapiro,²⁴ P. F. Shepard,³⁶ T. Shibayama,⁴⁵ M. Shimojima,⁴⁵
 M. Shochet,⁹ A. Sidoti,³³ J. Siegrist,²⁴ A. Sill,⁴² P. Sinervo,⁴³ P. Singh,¹⁹ A. J. Slaughter,⁴⁹ K. Sliwa,⁴⁶
 C. Smith,²⁰ F. D. Snider,¹² A. Solodsky,³⁹ J. Spalding,¹² T. Speer,¹⁵ P. Sphicas,²⁵ F. Spinella,³⁵ M. Spiropulu,⁹
 L. Spiegel,¹² J. Steele,⁴⁸ A. Stefanini,³⁵ J. Strolugas,¹⁹ F. Strumia,¹⁵ D. Stuart,¹² K. Sumorok,²⁵ T. Suzuki,⁴⁵
 T. Takano,³¹ R. Takashima,¹⁸ K. Takikawa,⁴⁵ P. Tamburello,¹¹ M. Tanaka,⁴⁵ B. Tannenbaum,⁶ M. Tecchio,²⁶
 R. J. Tesarek,¹² P. K. Teng,¹ K. Terashi,³⁹ S. Tether,²⁵ A. S. Thompson,¹⁶ E. Thomson,³⁰ R. Thurman-Keup,²
 P. Tipton,³⁸ S. Tkaczyk,¹² D. Toback,⁴¹ K. Tollefson,³⁸ A. Tollestrup,¹² D. Tonelli,³⁵ M. Tonnesmann,²⁷
 H. Toyoda,³¹ W. Trischuk,⁴³ J. F. de Troconiz,¹⁷ J. Tseng,²⁵ D. Tsybychev,¹³ N. Turini,³⁵ F. Ukegawa,⁴⁵
 T. Unverhau,¹⁶ T. Vaiciulis,³⁸ J. Valls,⁴⁰ E. Vataga,³⁵ S. Vejcik III,¹² G. Velev,¹² G. Veramendi,²⁴ R. Vidal,¹²
 I. Vila,⁷ R. Vilar,⁷ I. Volobouev,²⁴ M. von der Mey,⁶ D. Vucinic,²⁵ R. G. Wagner,² R. L. Wagner,¹² N. B. Wallace,⁴⁰
 Z. Wan,⁴⁰ C. Wang,¹¹ M. J. Wang,¹ S. M. Wang,¹³ B. Ward,¹⁶ S. Waschke,¹⁶ T. Watanabe,⁴⁵ D. Waters,³²
 T. Watts,⁴⁰ R. Webb,⁴¹ M. Webber,²⁴ H. Wenzel,²¹ W. C. Wester III,¹² A. B. Wicklund,² E. Wicklund,¹²
 T. Wilkes,⁵ H. H. Williams,³⁴ P. Wilson,¹² B. L. Winer,³⁰ D. Winn,²⁶ S. Wolbers,¹² D. Wolinski,²⁶
 J. Wolinski,²⁷ S. Wolinski,²⁶ S. Worm,⁴⁰ X. Wu,¹⁵ J. Wyss,³⁵ W. Yao,²⁴ G. P. Yeh,¹² P. Yeh,¹ J. Yoh,¹²
 C. Yosef,²⁷ T. Yoshida,³¹ I. Yu,²² S. Yu,³⁴ Z. Yu,⁴⁹ J. C. Yun,¹² A. Zanetti,⁴⁴ F. Zetti,²⁴ and S. Zucchelli³

(The CDF Collaboration)

¹*Institute of Physics, Academia Sinica, Taipei, Taiwan 11529, Republic of China*

²*Argonne National Laboratory, Argonne, Illinois 60439*

³*Istituto Nazionale di Fisica Nucleare, University of Bologna, I-40127 Bologna, Italy*

⁴*Brandeis University, Waltham, Massachusetts 02254*

⁵*University of California at Davis, Davis, California 95616*

⁶*University of California at Los Angeles, Los Angeles, California 90024*

⁷*Instituto de Fisica de Cantabria, CSIC-University of Cantabria, 39005 Santander, Spain*

⁸*Carnegie Mellon University, Pittsburgh, PA 15218*

⁹*Enrico Fermi Institute, University of Chicago, Chicago, Illinois 60637*

¹⁰*Joint Institute for Nuclear Research, RU-141980 Dubna, Russia*

¹¹*Duke University, Durham, North Carolina 27708*

¹²*Fermi National Accelerator Laboratory, Batavia, Illinois 60510*

¹³*University of Florida, Gainesville, Florida 32611*

¹⁴*Laboratori Nazionali di Frascati, Istituto Nazionale di Fisica Nucleare, I-00044 Frascati, Italy*

¹⁵*University of Geneva, CH-1211 Geneva 4, Switzerland*

¹⁶*Glasgow University, Glasgow G12 8QQ, United Kingdom*

¹⁷*Harvard University, Cambridge, Massachusetts 02138*

¹⁸*Hiroshima University, Higashi-Hiroshima 724, Japan*

¹⁹*University of Illinois, Urbana, Illinois 61801*

²⁰*The Johns Hopkins University, Baltimore, Maryland 21218*

²¹*Institut für Experimentelle Kernphysik, Universität Karlsruhe, 76128 Karlsruhe, Germany*

²²*Center for High Energy Physics: Kyungpook National University, Taegu 702-701; Seoul National University, Seoul 151-742; and SungKyunKwan University, Suwon 440-746; Korea*

²³*High Energy Accelerator Research Organization (KEK), Tsukuba, Ibaraki 305, Japan*

²⁴*Ernest Orlando Lawrence Berkeley National Laboratory, Berkeley, California 94720*

²⁵*Massachusetts Institute of Technology, Cambridge, Massachusetts 02139*

²⁶*University of Michigan, Ann Arbor, Michigan 48109*

²⁷*Michigan State University, East Lansing, Michigan 48824*

²⁸*University of New Mexico, Albuquerque, New Mexico 87131*

²⁹*Northwestern University, Evanston, Illinois 60208*

³⁰*The Ohio State University, Columbus, Ohio 43210*

³¹*Osaka City University, Osaka 588, Japan*

³²*University of Oxford, Oxford OX1 3RH, United Kingdom*

³³*Universita di Padova, Istituto Nazionale di Fisica Nucleare, Sezione di Padova, I-35131 Padova, Italy*

³⁴*University of Pennsylvania, Philadelphia, Pennsylvania 19104*

³⁵*Istituto Nazionale di Fisica Nucleare, University and Scuola Normale Superiore of Pisa, I-56100 Pisa, Italy*

³⁶*University of Pittsburgh, Pittsburgh, Pennsylvania 15260*

³⁷*Purdue University, West Lafayette, Indiana 47907*

³⁸*University of Rochester, Rochester, New York 14627*

³⁹*Rockefeller University, New York, New York 10021*

⁴⁰*Rutgers University, Piscataway, New Jersey 08855*

⁴¹*Texas A&M University, College Station, Texas 77843*

⁴²*Texas Tech University, Lubbock, Texas 79409*

⁴³*Institute of Particle Physics, University of Toronto, Toronto M5S 1A7, Canada*

⁴⁴*Istituto Nazionale di Fisica Nucleare, University of Trieste/ Udine, Italy*

⁴⁵*University of Tsukuba, Tsukuba, Ibaraki 305, Japan*

⁴⁶*Tufts University, Medford, Massachusetts 02155*

⁴⁷*Waseda University, Tokyo 169, Japan*

⁴⁸*University of Wisconsin, Madison, Wisconsin 53706*

⁴⁹*Yale University, New Haven, Connecticut 06520*

(Dated: June 11, 2002)

We report a measurement of the ratio of the bottom quark production cross section in antiproton-proton collisions at $\sqrt{s} = 630$ GeV to 1800 GeV using bottom quarks with transverse momenta greater than 10.75 GeV identified through their semileptonic decays and long lifetimes. The measured ratio $\sigma(630)/\sigma(1800) = 0.171 \pm .024 \pm .012$ is in good agreement with next-to-leading order (NLO) quantum chromodynamics (QCD).

PACS numbers: 13.85.Qk 12.38.Qk

I. INTRODUCTION

Hadroproduction of heavy quarks, such as the bottom (or b) quark, at proton-antiproton colliders is an area where one expects perturbative quantum chromodynamics (QCD) to provide accurate and reliable predictions. Because b quarks are light enough to be produced in sufficient quantities to enable high statistics measurements (unlike the heavier top quarks at the present time), they provide an excellent arena in which to test these predictions. It therefore came as a surprise that Tevatron measurements [1, 2, 3, 4, 5, 6, 7] of the b -quark cross section in antiproton-proton collisions at $\sqrt{s} = 1800$ GeV were substantially larger (roughly a factor of two) than predicted by next-to-leading order (NLO) QCD, particularly since the UA1 measurements at $\sqrt{s} = 630$ GeV did not seem to show such a marked departure from prediction [8].

This disagreement could indicate that NLO QCD is insufficient and that higher order calculations are needed. It could indicate that our heavy quark fragmentation models are insufficient, such as suggested in the paper of Cacciari, Greco and Nason [9] which discusses improvements in theoretical predictions from resummation and altering fragmentation functions. It could also be explained by more exotic processes. For example, Berger *et al.* [10] propose gluino pair production with a subsequent decay into a bottom quark and a light bottom squark. Since the assumed gluino mass is larger than the mass of the b quark, this process would turn on more slowly with energy than pure QCD production of $b\bar{b}$ pairs. This new physics process will depress the ratio of the b -quark cross section at 630 GeV relative to 1800 GeV by of order 10%.

To address this apparent discrepancy, the Tevatron ran for nine days at an energy of $\sqrt{s} = 630$ GeV to provide a sample of b quarks produced at this energy. Rather than

calculating the absolute cross section at both energies and comparing, we chose to calculate the ratio of cross sections at the two energies. Both experimentally and theoretically, many systematic uncertainties partially or completely divide out. In particular, the largest theoretical uncertainty is the choice of scale, and in predicting the ratio a consistent scale must be chosen at both energies: this reduces the theoretical uncertainty from a factor of two to approximately 15% for the ratio.

This analysis identifies b -quark candidates by searching for long-lived particles with a muon as a decay product, and from the ratio of the number of candidate events at the two energies, we compute the ratio of cross sections. While a differential cross section with respect to transverse momentum ($d\sigma(b)/dp_T$) would provide the best comparison with theory, we have neither the number of events nor the p_T resolution to make a differential measurement. Instead we report the b -quark cross section above a minimum transverse momentum, $p_T(\text{min})$. We adopt the convention that $p_T(\text{min})$ will be chosen so that 90% of our reconstructed and identified b quarks have a larger transverse momentum: for this analysis that is 10.75 GeV/ c .

In this analysis, we make the assumption that the fragmentation, decay, and detector response to a b quark of a given p_T is the same at the two energies. Certainly the decays should be the same. In principle, there might be a difference in fragmentation between 630 GeV and 1800 GeV due to the difference in velocities of the proton remnant. It is common to use Peterson [11] fragmentation (developed for e^+e^- collisions) in $\bar{p}p$ collisions, and one would expect that any energy-dependent fragmentation change would be smaller than the error introduced in going from lepton to hadron colliders. Additionally, any difference should be at its minimum for b 's at central rapidity (measured in this analysis) because they are farthest from the forward-going proton and antiproton remnants.

The CDF detector is described in detail elsewhere [12]; a brief discussion follows. In the CDF detector, a 51 cm long silicon vertex detector (SVX) [13], located immediately outside the beampipe, provides precise track re-

*Present address: University of California, Santa Barbara, California, 93106

construction in the plane transverse to the beam and is used to identify secondary vertices that can be produced by b and c quark decays. Because $p\bar{p}$ interactions are spread along the beamline with a standard deviation of about 30 cm, slightly more than half of the events originate from primary vertices inside the SVX fiducial region (this fraction is a function of beam energy). The momentum of charged particles is measured in the central tracking chamber (CTC), which sits inside a 1.4 T superconducting solenoidal magnet. Outside the CTC are electromagnetic and hadronic calorimeters arranged in a projective tower geometry, covering the pseudorapidity region $|\eta| < 4.2$ [14]. Surrounding the calorimeters, drift chambers in the region $|\eta| < 1.0$ provide muon identification. In this analysis, we restrict ourselves to muons in the most central region ($|\eta| < 0.6$), requiring muons detected in both the inner central muon chambers (CMU), located behind approximately five interaction lengths of material, and the outer central muon upgrade chambers (CMP) behind an additional 60 cm of steel.

II. DATA SELECTION

Our goal was to make the two datasets (630 GeV and 1800 GeV) as similar as possible. All the data were collected between December 1995 and February 1996. Therefore, changes to the detector configuration and time-dependent effects were minimized.

Both online and offline event selections were identical for the two beam energies. A three-level trigger selected events with a high transverse momentum muon for this analysis. A muon was identified by requiring a match between the extrapolated track as reconstructed in the CTC and track segments reconstructed in the muon chambers, taking into account multiple scattering of the muon. At Level 1, events were selected online by having at least one identified short track (called a “stub”, having at least two hits out of four possible) in the CMU muon chambers with confirming hits in the outer CMP muon chambers. At Level 2, events were required to have a 4.7 GeV/ c p_T two-dimensional (r - ϕ) track in the central tracker pointing at a stub in the CMU. At Level 3, events were selected that had a good 3-dimensional track with $p_T > 4.5$ GeV/ c pointing at muon stubs with at least three hits in both the CMU and CMP chambers. Offline, the muon candidate was required to pass tight track-stub matching requirements: the momentum-dependent matching χ^2 must have been less than 9 in the x -direction for both CMU and CMP, and must have been less than 12 in the z -direction for CMU. The χ^2 variables were calculated for one degree of freedom. The muon track was required to have $p_T > 5.0$ GeV/ c as well as to have at least 3 (of 4 possible) hits in the SVX. For muons with p_T above 6 GeV/ c , the trigger efficiency is essentially constant (variation less than 1% with p_T). Monte Carlo calculations indicate 90 percent of the b quarks passing these requirements have transverse mo-

menta above 10.75 GeV/ c .

Much of the 1800 GeV sample had the 4.7 GeV/ c Level 2 muon trigger dynamically prescaled. At high luminosities, these triggers were run with a very high prescale factor (100 or more), and as the luminosity decreased, the prescale factors were lowered until the trigger ran with no prescale. This strategy maximizes the number of events recorded to tape, but complicates the calculation of the live luminosity. We elected to use the data itself to make this calculation. (Run-by-run bookkeeping yields a consistent result.) We looked at muon events that passed an unprescaled 12 GeV/ c muon trigger and we subjected them to the same offline cuts used for our sample, except that the minimum p_T was required to be 15 GeV/ c . Every one of these events should have passed the unprescaled 4.7 GeV/ c muon trigger, so this sample allows us to determine the effective prescale factor. We have 3943 such events, of which 1282 pass the prescaled trigger: our raw luminosity must therefore be multiplied by a prescale correction of 0.3250 ± 0.0075 . Applying this effective prescale and the luminosity systematic uncertainty of 4.2% [15], we get an effective integrated luminosity of 623 ± 30 nb $^{-1}$ at 1800 GeV.

At 630 GeV, this trigger had no prescale applied, and we collected an integrated luminosity of 582 ± 24 nb $^{-1}$.

The uncertainties on the integrated luminosities are independent, so the uncertainty on the ratio is straightforward to calculate. We obtain the ratio:

$$\frac{\mathcal{L}(630)}{\mathcal{L}(1800)} \equiv \frac{\int \mathcal{L} dt(630)}{\int \mathcal{L} dt(1800)} = 0.934 \pm .060.$$

III. b FINDING ALGORITHM

To identify b hadrons, we begin with a muon as a seed. We then select tracks with $p_T > 1.0$ GeV/ c in a cone of $R \equiv (\Delta\eta^2 + \Delta\phi^2)^{1/2} < 1.0$ and we require that the invariant mass of the muon-track combination be below 5.3 GeV/ c^2 when the track is assumed to be a pion. From this sample we select the track with the highest p_T . The track and muon are fit to the constraint that they come from a common point. Events with a fit χ^2 -based probability greater than 1% are selected if they also possess a secondary vertex within 2 cm of the primary vertex in the transverse plane. The number of b hadrons is proportional to the number of events with the two-track vertex ahead of the primary vertex (a sample composed of bottom hadrons plus mismeasured tracks) less the number with the two-track vertex behind the primary vertex (a sample composed predominantly of mismeasured tracks). In this context, “ahead” means that the secondary vertex displacement r is in the direction of the momentum vector of the bottom candidate and “behind” means that the secondary vertex displacement is opposite the direction of the momentum vector. We require the transverse flight distance ($L_{xy} \equiv r \cdot \hat{p}_T$) of a b candidate to exceed 250 μm ,

and the background sample to have $L_{xy} < -250 \mu\text{m}$. Vertices with small $|L_{xy}|$ are dominated by prompt particles.

Monte Carlo studies show that a few percent of real bottom hadrons are reconstructed in the $-L_{xy}$ sample, that is, behind the primary vertex. This exact fraction varies somewhat with different production models, most likely because of the different ΔR and $\Delta\phi$ distributions between the b and \bar{b} hadrons. However, a common feature of all Monte Carlos is that this fraction is the *same* at both 630 GeV and 1800 GeV, so the procedure outlined above still produces an accurate ratio of the number of events produced from collisions at 630 GeV and 1800 GeV.

To reduce the contamination in our sample from charm hadrons, we require the two-particle mass to be greater than $1.5 \text{ GeV}/c^2$, where we assume the second track is a pion. This is a very tight cut, being at the kinematic limit of charm decays, and rejects approximately half the $b \rightarrow \mu h^\pm X$ events. There are also indications of a high background level (for example, same-sign dimuons) in the low-mass sample. ISAJET [16] Monte Carlo studies show negligible charm contamination after these selection requirements.

This algorithm differs from the ones used in our top quark analyses, because the algorithms are designed to do quite different things: our top quark analysis is designed to identify b 's in a relatively b -poor sample, whereas this algorithm is designed to accurately count b 's in a relatively b rich sample, with significant c -contamination.

IV. RELATIVE ACCEPTANCE CALCULATION

To calculate the relative acceptance of the detector at the two different energies, two Monte Carlo datasets were created for this analysis, one simulating data at $\sqrt{s} = 630 \text{ GeV}$ and the other at $\sqrt{s} = 1800 \text{ GeV}$. Both use the MRSA' parton distributions and a renormalization scale of $\mu_0 \equiv \sqrt{m_b^2 + p_T^2}$.

Ten million events were generated at each energy and for a variety of parton distributions using a b -quark Monte Carlo with minimum b quark p_T of $6.75 \text{ GeV}/c$ and $|y| \leq 1$ and then fragmented using Peterson [11] fragmentation with $\epsilon = 0.006$. The $6.75 \text{ GeV}/c$ point was chosen because in a sample 10% this size, no events passing our selection requirements had a parent b quark with transverse momentum below this value. Bottom hadron decays were then simulated with version 9.0 of the CLEO B Decay Monte Carlo [17], using the standard decay tables. No decays (for instance $b \rightarrow \mu + X$) were forced, as $b \rightarrow c \rightarrow \mu$ is about 5% of the total acceptance at 630 GeV, and 18% of the total acceptance at 1800 GeV. Forcing the b to decay directly to muons would skew the results.

Events with a muon with a transverse momentum of at least $4.0 \text{ GeV}/c$ were then simulated using a fast detector simulation, and events with a muon candidate with a

TABLE I: Quantities used to determine the silicon vertex detector acceptance.

	1800 GeV	630 GeV
N_μ (all)	57882	28444
N_μ (with SVX track)	37825	14213
N_μ^* (all)	13891	5913
N_μ^* (with SVX track)	13219	5268

transverse momentum of $5.0 \text{ GeV}/c$ or greater were kept for further analysis.

The number of Monte Carlo events in the 1800 GeV sample passing all cuts is 4045 ± 67 after subtraction of events with negative L_{xy} , and the equivalent number in the 630 GeV sample is 2850 ± 56 . The relative acceptance A_{630}/A_{1800} is therefore 0.705 ± 0.018 .

A correction to this is necessary as the SVX acceptance in the two datasets is not identical. The 630 GeV run had the Tevatron's final focus running at a nominal β^* of approximately 75 cm rather than the usual value at 1800 GeV of 35 cm, which widened the z distribution of collisions, causing more events to fall outside of the SVX acceptance. Additionally, the mean primary vertex position was shifted with respect to the 1800 GeV data.

We measured the acceptance from the data by looking at good CTC tracks and asking how often a good SVX track is associated with it. In particular, we use muons that pass all the cuts in this analysis although for calculating the acceptance we do not care if they are part of a b candidate or not.

We calculate the relative acceptance for the SVX in the following way:

$$A_{630/1800} = \frac{(N_\mu(SVX)/N_\mu)_{630} (N_\mu^*(SVX)/N_\mu^*)_{1800}}{(N_\mu(SVX)/N_\mu)_{1800} (N_\mu^*(SVX)/N_\mu^*)_{630}}$$

The unstarred quantities are the number of muons in the entire luminous region, and the starred quantities are the number of muons in the region where the SVX efficiency and acceptance are at their largest (the region where the vertex z -position is between 10 and 20 cm on both the east and west sides). This calculation is done to decouple the SVX reconstruction probability from the difference in acceptance due to the differing beam profile. This probability may be different for muons from π and K decays than for prompt muons and muons from heavy flavor decays, and the muon sample composition may differ at the two energies. This technique divides out this effect so that only the geometric factor remains. This approach is equivalent to taking the 1800 GeV SVX efficiency curve and superimposing it on the 630 GeV beam profile. The measured values are shown in Table I. We calculate a relative acceptance factor due to the beam profile of 0.817 ± 0.014 .

The Monte Carlo dataset used in the acceptance calculation was generated with $p_T(b) > 6.75 \text{ GeV}/c^2$ to fully populate the p_T spectrum, but the convention is

TABLE II: Number of candidate events at each energy.

	1800 GeV	630 GeV
Luminosity (nb^{-1})	628 ± 30	582 ± 24
Events $L_{xy} > 250 \mu\text{m}$	3083	383
Events $L_{xy} < -250 \mu\text{m}$	1527	200
Forward Excess	1556 ± 68	183 ± 24

to quote the cross section above a $p_T(\text{min})$ such that 90% of the reconstructed b quarks have $p_T > p_T(\text{min})$. For this analysis $p_T(\text{min})$ is $10.75 \text{ GeV}/c$. Because of the different p_T spectra at the two energies, Monte Carlo datasets that have the same number of entries for $p_T(b) > 6.75 \text{ GeV}/c$ will not have the same number of entries for $p_T(b) > 10.75 \text{ GeV}/c$, so an additional correction factor of 1.282 ± 0.007 is necessary. The uncertainty was obtained by varying the scale from μ_0 to $\mu_0/2$ and $2\mu_0$ and varying b quark mass from $4.75 \text{ GeV}/c^2$ to 4.5 and $5.0 \text{ GeV}/c^2$. Combining all these factors yields a total relative acceptance $A_{630}/A_{1800} = 0.738 \pm 0.023$.

A number of studies were made to insure the stability of this result: we verified that gluon splitting to $c\bar{c}$ does not affect this result, nor is it sensitive to the fraction of b 's produced by gluon splitting rather than $2 \rightarrow 2$ processes. We also verified that the algorithm's choice of fragmentation tracks over b daughters is the same at both energies. Finally, we verified that changing the track selection algorithm leaves the ratio of cross sections unchanged, and we verified that we were insensitive to the value of b quark lifetime when we varied $c\tau$ between 400 and $500 \mu\text{m}$.

V. RESULTS

A. b Quark Counting

The L_{xy} distributions at 1800 GeV and 630 GeV are shown in Figures 1 and 2 respectively. As shown in Table II in the 1800 GeV sample, there are 3083 events at least $250 \mu\text{m}$ ahead of the primary vertex and 1527 events at least $250 \mu\text{m}$ behind the primary vertex, yielding a forward excess of 1556 ± 68 events. In the 630 GeV sample, there are 383 events at least $250 \mu\text{m}$ ahead of the primary vertex and 200 events at least $250 \mu\text{m}$ behind the primary vertex, yielding a forward excess of 183 ± 24 events.

The ratio of observed b -quark candidate events (before correcting for acceptance) is therefore given by:

$$\frac{N_{630}/\mathcal{L}_{630}}{N_{1800}/\mathcal{L}_{1800}} = 0.126 \pm .020.$$

B. Relative Cross Section

The relative cross section is given by:

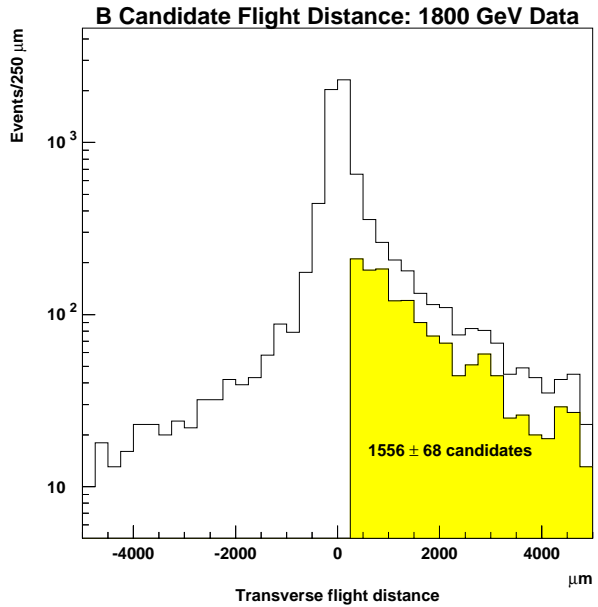


FIG. 1: The transverse flight distance distribution for b candidates at $\sqrt{s} = 1800 \text{ GeV}$. The shaded region is the excess at large positive L_{xy} .

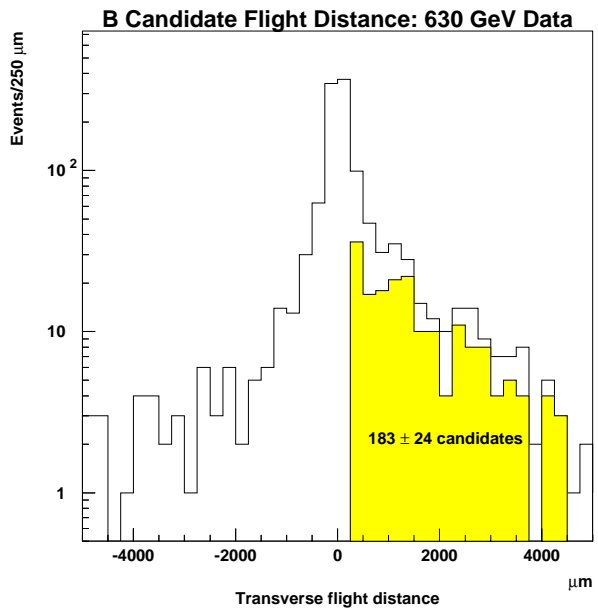


FIG. 2: The transverse flight distance distribution for b candidates at $\sqrt{s} = 630 \text{ GeV}$. The shaded region is the excess at large positive L_{xy} .

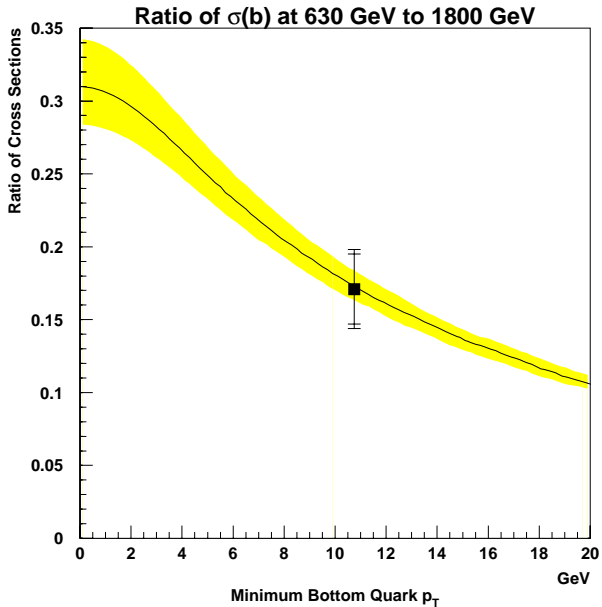


FIG. 3: The ratio of $\sigma(b)$ at $\sqrt{s} = 630$ GeV to $\sqrt{s} = 1800$ GeV as a function of the minimum b -quark transverse momentum, $p_T(\text{min})$. The inner error bars are statistical only, and the outer ones include systematic uncertainties as well. This is compared to the NLO QCD prediction using MRSA' parton distributions; the central value is obtained with a b -quark mass of 4.75 GeV/ c^2 and a renormalization scale of $\mu_0 = \sqrt{m_b^2 + p_T^2}$. The shaded region covers the variation obtained by varying the scale between $\mu_0/2$ and $2\mu_0$ and the mass between 4.5 and 5.0 GeV/ c^2 .

$$\frac{\sigma_b(p_T > 10.75)_{630}}{\sigma_b(p_T > 10.75)_{1800}} = \frac{N_b(630)/N_b(1800)}{A_b(630)/A_b(1800)\mathcal{L}(630)/\mathcal{L}(1800)}$$

which, when all the factors are put in, yields

$$\frac{\sigma_b(p_T > 10.75)_{630}}{\sigma_b(p_T > 10.75)_{1800}} = 0.171 \pm .024 \pm .012$$

where the first uncertainty is statistical and the second is systematic.

The theoretical prediction of NLO QCD [8, 18] using MRSA' parton distributions [19] is $0.174 \pm .011$. The uncertainty was obtained by varying the renormalization scale from μ_0 to $\mu_0/2$ and $2\mu_0$ and by varying the b quark mass from 4.75 GeV/ c^2 to 4.5 and 5.0 GeV/ c^2 . Our results are compared to NLO QCD predictions using MRSA' and MRST [20] parton distributions in Figures 3 and 4 respectively.

We can combine this with our measured B meson cross section at 1800 GeV [1] and fragmentation ratios [21] to

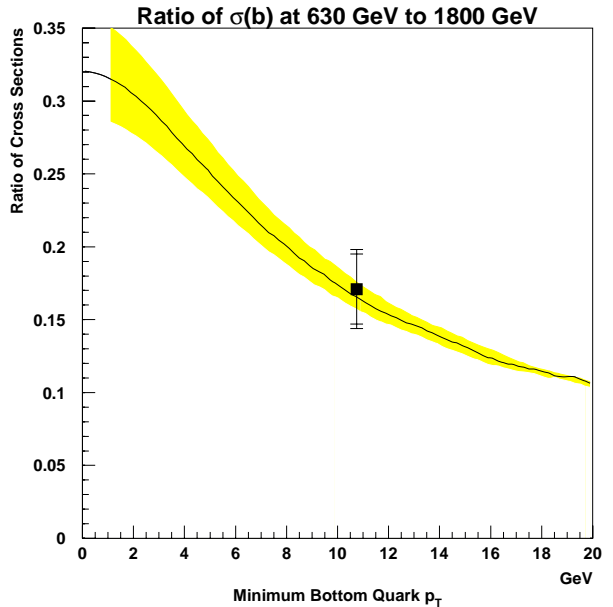


FIG. 4: The ratio of $\sigma(b)$ at $\sqrt{s} = 630$ GeV to $\sqrt{s} = 1800$ GeV as a function of the minimum b -quark transverse momentum, $p_T(\text{min})$. The inner error bars are statistical only, and the outer ones include systematic uncertainties as well. This is compared to the NLO QCD prediction using MRST parton distributions; the central value is obtained with a b -quark mass of 4.75 GeV/ c^2 and a renormalization scale of $\mu_0 = \sqrt{m_b^2 + p_T^2}$. The shaded region covers the variation obtained by varying the scale between $\mu_0/2$ and $2\mu_0$ and the mass between 4.5 and 5.0 GeV/ c^2 .

obtain a cross section at 630 GeV which can be compared directly with the results from the UA1 experiment [22]. This is shown in Figure 5.

VI. CONCLUSIONS

The ratio of the b -quark cross sections at 630 and 1800 GeV matches well with the QCD prediction. Interpreting this as an absolute cross-section measurement at 630 GeV shows our measurement above the UA1 value, but not so far above that the measurements would be inconsistent at the 95% confidence level. The large b -quark cross section is not something that is specific to 1800 GeV data. It is interesting to note that NLO QCD predictions using modern parton distributions tend to be below the most recent UA1 points as well, although at a level consistent with their uncertainties.

Acknowledgments

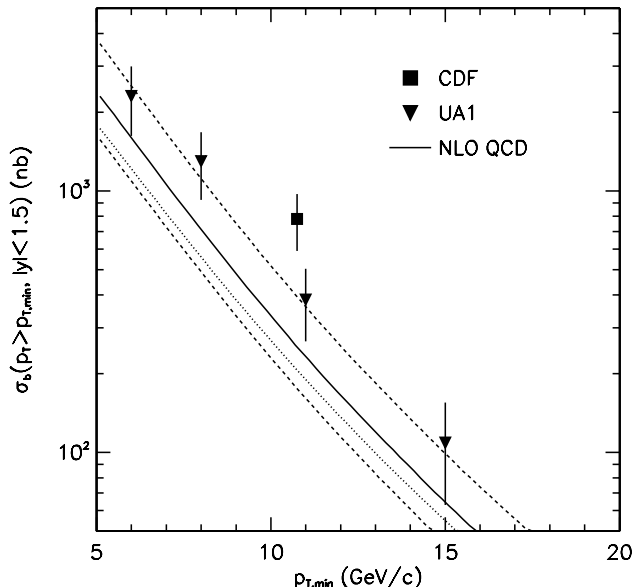


FIG. 5: The b quark cross section at 630 GeV for CDF and UA1. The solid line is the NLO QCD prediction using MRST parton distributions using a renormalization scale of $\mu_0 = \sqrt{m_b^2 + p_T^2}$. The dashed lines cover a scale variation between $\mu_0/2$ and $2\mu_0$ and a b -quark mass variation between $4.5 \text{ GeV}/c^2$ and $5 \text{ GeV}/c^2$. The dotted line is the equivalent of the solid line except with MRSA' parton distributions.

We thank the Fermilab staff and the technical staffs of the participating institutions for their vital contributions. This work was supported by the U.S. Department of Energy and National Science Foundation; the Italian Istituto Nazionale di Fisica Nucleare; the Ministry of Education, Culture, Sports, Science, and Technology of Japan; the Natural Sciences and Engineering Research Council of Canada; the National Science Council of the Republic of China; the Swiss National Science Foundation; the A. P. Sloan Foundation; the Bundesministerium fuer Bildung und Forschung, Germany; the Korea Science and Engineering Foundation (KoSEF); the Korea Research Foundation; and the Comision Interministerial de Ciencia y Tecnologia, Spain.

-
- [1] F. Abe *et al.* Phys. Rev. Lett. **75**, 1451 (1995).
[2] F. Abe *et al.* Phys. Rev. D **53**, 1051 (1996).
[3] F. Abe *et al.* Phys. Rev. D **50**, 4252 (1994).
[4] D. Acosta *et al.* Phys. Rev. D **65**, 052005 (2002).
[5] S. Abachi *et al.* Phys. Rev. Lett. **74**, 3548 (1995).
[6] B. Abbott *et al.* Phys. Lett. B **487**, 264 (2000).
[7] B. Abbott *et al.* Phys. Rev. Lett. **85**, 5068 (2000).
[8] P. Nason, S. Dawson, R. K. Ellis, Heavy Quark Production In Hadronic Collisions," Nucl. Phys. B **327**, 49 (1989) [Erratum-ibid. B **335**, 260 (1989)].
[9] M. Cacciari, M. Greco, P. Nason, JHEP **9805**, 007 (1998).
[10] E. L. Berger, B. W. Harris, D. E. Kaplan, Z. Sullivan, T. M. Tait and C. E. Wagner, Phys. Rev. Lett. **86**, 4231 (2001).
[11] C. Peterson *et al.*, Phys. Rev. D **27**, 105 (1983).
[12] F. Abe *et al.*, Nucl. Instrum. Meth. A **271**, 387 (1988); F. Abe *et al.*, Report No. FERMILAB-PUB-94/097-E.
[13] D. Amidei *et al.*, Nucl. Instrum. Meth. A **350**, 73 (1994); P. Azzi *et al.*, Nucl. Instrum. Meth. A **360**, 137 (1995).
[14] In the CDF coordinate system, θ and ϕ are the polar and azimuthal angles, respectively, defined with respect to the proton beam direction z . The pseudorapidity η is defined as $-\ln \tan(\theta/2)$. The transverse momentum of a particle is $p_T = p \sin(\theta)$.
[15] D. Cronin-Hennessy, A. Beretvas and P. F. Derwent, Nucl. Instrum. Meth. A **443**, 37 (2000). Note that this uncertainty is somewhat smaller than what is usually quoted by CDF. This is because this is only the component of the luminosity uncertainty that is not in common between the measurements at 1800 GeV and 630 GeV.
[16] F. Paige and S. Protopopescu, Brookhaven National Laboratory Report No. BNL-38034, 1986 (unpublished).
[17] P. Avery, K. Read and G. Trahern, CLEO Report No, CSN-212 1985, (unpublished).
[18] P. Nason, S. Dawson and R. K. Ellis, Nucl. Phys. B **303** 607 (1988).
[19] A. D. Martin, R. G. Roberts and W. J. Stirling, Phys. Lett. B **354**, 155 (1995).
[20] A. D. Martin, R. G. Roberts, W. J. Stirling and R. S. Thorne, Eur. Phys. J. C **4**, 463 (1998).
[21] F. Abe *et al.* Phys. Rev. D **60**, 092005 (1999).
[22] C. Albajar *et al.*, Z. Phys. C **61**, 41 (1994).